Fluid-Mineral Interactions: A Tribute to H. P. Eugster
© The Geochemical Society, Special Publication No. 2, 1990
Editors: R. J. Spencer and I-Ming Chou

Partitioning of base metals between silicates, oxides, and a chloride-rich hydrothermal fluid. Part I. Evaluation of data derived from experimental and natural assemblages

EUGENE S. ILTON

Department of Mineral Sciences, American Museum of Natural History, Central Park West at 79th St., New York, New York 10024, U.S.A.

and

HANS P. EUGSTER

Department of Earth and Planetary Sciences, The Johns Hopkins University, Baltimore, Maryland 21218 U.S.A.

Abstract—Exchange reactions for base metals between common Fe-Mg silicates, oxides and a chloride-rich hydrothermal/metamorphic fluid were calibrated by combining experimentally determined apparent equilibrium constants (*Kd*(magnetite/fluid) and *Kd*(biotite/fluid)) with apparent mineral/magnetite-biotite equilibrium constants derived from natural assemblages and experiments.

The resulting distribution coefficients suggest that the rock-forming silicates and oxides will preferentially partition (Cu > Cd) ≫ Zn ≫ Mn ≫ Fe ≫ Mg into the fluid phase. The results for copper and cadmium are bracketed to indicate that they are statistically inconclusive, but suggestive of potentially strong fractionation.

INTRODUCTION

A MAJOR PROBLEM concerning the formation of hydrothermal ore deposits involves the manner and timing of metal enrichment. Enrichment can occur at any stage, from the formation of the source rock or magma to the depositional event. It has become apparent, however, that hydrothermal ore deposits need not be associated with source rocks or magmas that have anomalously high concentrations of metals. SKINNER (1979) states: ". . . any rock can serve as a source of geochemically scarce metals provided a hydrothermal solution undergoes the reactions that will extract them."

This contribution attempts to elucidate the role of exchange reactions in the enrichment of manganese, zinc, copper, and cadmium during the interaction of hydrothermal/metamorphic fluids with common rock-forming silicates and oxides. Iron serves as the standard of comparison because the base metals of interest may be expected to form solid solutions with iron; the oxidation states and ionic radii of Mn^{2+}, Zn^{2+}, and Cu^{2+} are similar to those of Fe^{2+}, and HAACK *et al.* (1984) and HEINRICHS *et al.* (1980) have suggested that cadmium is associated with the Fe^{2+}-bearing silicates. Since iron is considerably more abundant than zinc, manganese, cadmium, and copper, the manner in which these minor-trace metals become enriched relative to iron poses a significant problem. The relevant partition coefficients are derived here in Part I, and applied in Part II (this volume).

There are a variety of geochemical approaches to the study of base metal enrichment: partitioning experiments (mineral/fluid—ILTON and EUGSTER, 1989; melt/fluid—HOLLAND, 1972; CANDELA and HOLLAND, 1984), solubility experiments (see reviews by BARNES, 1979; EUGSTER, 1986), whole-rock/fluid interaction experiments (*e.g.*, ELLIS, 1968; BISCHOFF and DICKSON, 1975; HAJASH, 1975; MOTTL *et al.*, 1979; SEYFRIED and BISCHOFF, 1981; SEYFRIED and MOTTL, 1982; SEYFRIED and JANECKY, 1985), theoretical predictions of solid/fluid metal partitioning (SVERJENSKY, 1984, 1985), studies of fluid inclusions (review by ROEDDER, 1984), and observations of modern geothermal and hydrothermal fluids (review by WEISSBERG *et al.*, 1979; HENLEY and ELLIS, 1983).

Experimental results for Zn-Fe, Mn-Fe, Cu-Fe and Cd-Fe partitioning between magnetite and a supercritical (H_2O-KCl) solution (ILTON and EUGSTER, 1989) imply very strong partitioning of zinc and manganese into the fluid phase relative to iron and even stronger partitioning of copper and cadmium into the fluid relative to zinc and manganese. Preliminary experiments indicate that biotite strongly partitions zinc into the fluid relative to iron (ILTON, 1987). The results are applicable in a variety of geological environments since magnetite occurs in ultramafic to granitic igneous rocks and in different grades and compositions of metamorphic rocks.

This paper generalizes the results of ILTON and

EUGSTER (1989), and ILTON (1987) by deriving $Kd(\text{fl/min}) = (M/\text{Fe})^{\text{fl}}/(M/\text{Fe})^{\text{min}}$, where M represents the metal of interest, and the superscripts fl and min represent the fluid and mineral of interest, respectively, by combining Kd(fl/mt) and Kd(fl/biot) with magnetite-biotite/mineral distribution coefficients from natural rocks and mineral/mineral exchange experiments. The method has been described by EUGSTER and ILTON (1983).

This simple empirical approach provides information concerning the influence of the rock-forming silicates and oxides on the relative mobility of base metals for a variety of rock environments. Derived Kds(fl/min) should be considered preliminary order-of-magnitude calculations. Uncertainties in temperature estimates and compositional differences between experimental and natural assemblages increase the uncertainty of the calculations. Uncertainties due to pressure estimates and extrapolations, however, are considered relatively minor. Moreover, derived Kds(fl/min) may be appropriate only for fluids that are similar to the fluid in the fl/mt-biot experiments (*i.e.*, Cl_T = 2 molal, P = 2 kb, fO_2 = NNO), and for minerals with compositions near those used in the derivations. Because the partition coefficients for Mn-Fe and Zn-Fe involve the *ratios* of similar metals, the partition coefficients will be valid over the range of fluid compositions where metal speciation is similar and γ_M/γ_{Fe} is constant or near unity. This condition may occur in the lower pressure, higher temperature portion of the supercritical region where metal chloride speciation tends towards neutral complexes (*i.e.*, the experimental conditions, see discussion in ILTON and EUGSTER, 1989).

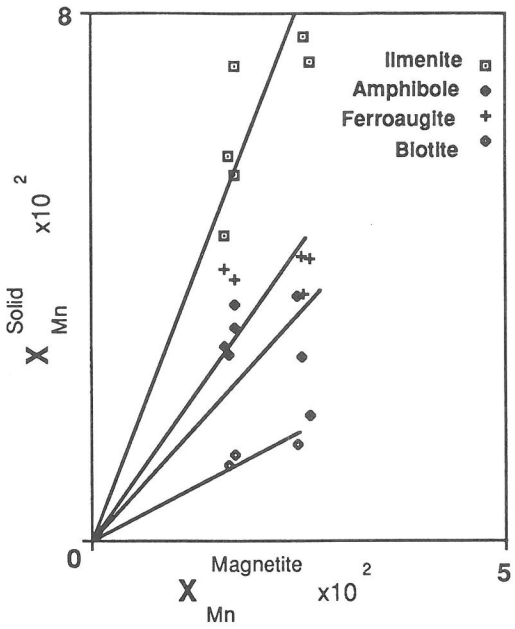

FIG. 1. Mole fraction diagram illustrating Mn-Fe^{2+} partitioning, at ~700°C, between magnetite and the minerals ilmenite, ferroaugite, amphibole, and biotite. The solid lines mark mean Kd for each mineral. The compositions of the minerals are reported as the mole fraction X_{Mn} = Mn/(Mn + Fe^{2+}). Mineral compositions are from FERRY (1985b).

HOST MINERALS FOR Mn, Zn, Cu AND Cd

The importance of a mineral as a host for an element depends on the minerals abundance and its affinity for a particular element. The dominant host for a given element changes from rock to rock as a function of mineral modes, composition, pressure and temperature. In many rock types, the bulk of the whole-rock manganese and zinc is contained in the rock-forming ferromagnesian silicate fraction. Olivine and pyroxene are the dominant hosts for manganese in ultramafic to mafic rocks, whereas hornblende and biotite are the dominant hosts for manganese *and* zinc in more felsic rocks. Unlike manganese, the dominant host for zinc in basaltic rocks is magnetite (WEDEPOHL, 1972). Hydrothermal alteration introduces other important hosts for manganese and zinc such as chlorite and serpentine. In metamorphic rocks, garnet and staurolite become important hosts for manganese and zinc respectively, as do amphibole, biotite and chlorite.

The low concentrations of cadmium in average crustal rock pose a significant problem for identifying its dominant hosts. DISSANAYAKE and VINCENT (1972), and HEINRICHS *et al.* (1980) give the fraction of whole-rock cadmium held in specific silicates and oxides in their tables VI and 3, respectively. Such work suggests that the silicate-oxide fraction is the dominant host for cadmium. Alternatively, it is possible that cadmium might occur mainly in the sulfide fraction (MAROWSKY and WEDEPOHL, 1971).

It is possible that copper is mainly present as sulfides in geological environments. HASLAM (1968) presents mineral modes and whole rock and mineral analyses for copper from a suite of granodiorites to granites. Among the ferromagnesium-silicates, biotite carries most of the whole rock copper. Most of the samples, however, indicate that silicates only account for ⅓ or less of the whole rock copper. Calculations using data from DE ALBUQUERQUE (1971, 1973) indicate that biotite, for the most part, accounts for ⅓ or less of the whole rock copper. Data from GRAYBEAL (1973) indicate that chlorite + biotite + hornblende account for roughly 50% of the whole rock copper in granodiotites associated with porphyry copper deposits.

Considering that the cleanest silicate separate may contain inclusions of sulfide minerals and alteration products (*e.g.*, BANKS, 1974), the above calculations are consistent with the commonly-held belief that sulfides are indeed the dominant copper hosts. Further complications are discussed later, and in ILTON and VEBLEN (1988a and 1988b). Regardless, numerous workers have suggested that silicates such as biotite are sources of copper in porphyry copper systems (*e.g.*, GRAYBEAL, 1973; HENDRY *et al.*, 1981). Models of copper transport that involve the oxide-silicate rock fraction as copper hosts may be useful to test the degree of sulfide control on the mobility and fractionation of copper in metasomatic systems.

Table 1. List of values for $Kd = (Mn/Fe^{2+})^{min}/(Mn/Fe^{2+})^{mt}$

	800°C	725°C	700°C			500°C
	B	Hd	F	B	P	F′
calcite						1.8 **
garn/ilm					5.05 ± 0.54 (±0.45)	
ilmenite		2.04 ± 0.18 (±0.07)	3.47 ± 0.24 (±0.20)			
cpx	2.02 1.5–2.6		1.97 ± 0.49 (±0.61)	4.49 3.3–5.8		
amphibole			1.55 ± 0.49 (±0.45)			11.8 ± 1.8 *
talc						6.98 ± 5.45 *
chlorite						6.63 ± 4.94 *
biotite		0.527 ± 0.125 (±0.080)	0.652 ± 0.085 (±0.212)			2.20 **

Errors are reported as one standard deviation. The 95% confidence intervals, calculated from the students *t* distribution, are bracketed. Errors for cpx data from Burton given as range. Mineral compositions from B: BURTON *et al.* (1982); P: POWNCEBY *et al.* (1987); F: FERRY (1985b); F′: FERRY (1985a); Hd: HILDRETH (1977).

* Small sample sizes, 95% confidence interval exeeds 100% of partition coefficient.

** Only one sample.

The preceeding discussion highlights the need for a general understanding of mineral/fluid exchange reactions. Given numerous *Kds*(mineral/fluid) it should be possible to model the exchange of base metals between hydrothermal fluids and a variety of rock types.

ERROR ANALYSIS

Standard deviations and 95% confidence intervals are given with each intermineral partition coefficient. Uncertainties associated with *Kd*(fl/min) are calculated by propagating the errors associated with *Kd*(fl/mt-biot) and *Kd*(mt-biot/min). Small sample sizes required the use of the students *t* distribution for calculating 95% confidence intervals.

Uncertainties associated with temperature estimates, the degree of equilibrium attained in natural and experimental assemblages, and compositional differences between experimental assemblages and natural assemblages are noted and qualitatively assessed.

The appendix contains more detailed petrographic information and assessments of equilibrium.

Mn-Fe PARTITIONING

In geological environments at higher *P* and *T*, manganese is commonly restricted to the divalent state (WEDEPOHL, 1978). One should expect Mn^{2+} to substitute preferably for Fe^{2+} since the majority of the crystal chemical properties of Mn^{2+} are closer to those of Fe^{2+} than Mg^{2+} or Ca^{2+}. Accordingly, when sufficient data has been provided, reactions are formulated as Mn-Fe^{2+} exchanges, where $Kd = (Mn/Fe^{2+})^{A}/(Mn/Fe^{2+})^{B}$. Intermineral partition coefficients are listed in Tables 1 and 2. More detailed petrographic information for each assemblage is located in the appendix.

FERRY (1985b) provides mineral analyses of coexisting magnetites, ilmenites, biotites, amphiboles, and ferroaugites in granites from the Isle of Skye. Calculated distribution coefficients, *Kd*(min/mt), are illustrated in Fig. 1 and listed in Table 1. Whereas the data indicate that the partitioning behavior of these minerals vary, the range of compositions are too narrow for speculations concerning attainment of equilibrium. The minerals, in the samples used, have compositions that record temperatures in the range 670–720°C.

POWNCEBY *et al.* (1987) experimentally calibrated Mn-Fe partitioning between ilmenite and garnet (alm-spess solid solutions) from 900–600°C, 2–5 kb, and over a wide range of Mn/(Mn + Fe) bulk compositions. *Kd*(garn/ilm) values were neither significantly dependent on pressure nor, for the purposes of this paper, on composition. The experiments closely bracketed equilibrium at all temperatures. *Kd*(garn/ilm), at 700°C, is given in Table 1.

Combining, at 700°C, *Kds*(min/mt) from FERRY (1985b) and *Kd*(garn/ilm) from POWNCEBY *et al.* (1987), with *Kd*(mt/fluid) given by ILTON and EUGSTER (1989) yields a host of mineral-fluid exchange reactions. The results are listed in Table 3. Given the precision of the data, we conclude that

Table 2. List of values for $Kd = (M/Fe)^{min\ A}/(M/Fe)^{min\ B}$ at ~500°C, where M is the moles of the metal of interest

	Mn-Fe		Zn-Fe		Cu-Fe		Cd-Fe
			1	2	1	2	
biot/mt	25.3 ± 17.1 (±13.2)		109 ± 227 (±162)	23 ± 19 (±16)	22 ± 29 (±22)	9.1 ± 8.7 (±7.3)	10.1 ± 9.2 (±6.3)
	AC	H					
amph/mt	51.5 ± 23.9 (±25.1)	22.5 ± 4.9 (±12.2)	17.3 ± 15.9 (±12.2)		6.8 ± 5.8 (±4.5)		13.5 ± 12.9 (±10.7)
biot/amph			1.72 ± 1.06 (±0.89)		1.30 ± 1.43 (±1.20)		0.39 ± 0.23 (±0.19)

All values derived from mineral compositions in ANNERSTEN and EKSTROM (1971). Errors are reported as one standard deviation. The 95% confidence intervals, calculated from the students t distribution, are bracketed. AC—actinolite; H—hornblende. See text for a discussion of values 1 and 2.

Mn-Fe partitioning between minerals and fluid varies greatly. This implies that given the same whole rock Mn/Fe ratios, mineralogically different rock types can impart vastly different Mn/Fe ratios to the fluid. Note that garnet might partition iron into the fluid relative to manganese!

These numbers should be considered order-of-magnitude calculations due to imperfect temperature estimates, lack of criteria that prove equilibrium, and possible compositional controls. The compositions of natural magnetites are perhaps critically important. The major component other than Fe_3O_4 in the magnetites is Fe_2TiO_4 (FERRY, 1985b), with the concentration of TiO_2 varying from 8–15 wt%. Charge balance effects were accounted for by formulating Mn-Fe^{2+} exchange reactions.

HILDRETH (1977, 1979) reports mineral compositions from the high silica rhyolites of the Bishop Tuff over a T range 720–790°C. Magnetite, ilmenite, and biotite compositions, for T = 720–730°C, are similar to those from FERRY (1985b), and are plotted in Fig. 2. Figure 2 reveals a strong correlation between X_{Mn} in ilmenite and X_{Mn} in magnetite, consistent with exchange equilibrium. Biotite/magnetite Mn-Fe^{2+} partitioning displays a similar correlation, also consistent with exchange equilibrium (see Fig. 2). Kd(ilm-biot/mt) values are given in Table 1. Values for Kd(fl/ilm) and Kd(fl/biot), listed in Table 3, were derived from the low temperature data (720–730°C) using Kd(fl/mt) at 725°C.

Results derived from a plutonic environment (FERRY, 1985b) are consistent with results from an extrusive environment (HILDRETH, 1977; 1979) where exchange equilibrium has been better demonstrated.

ANNERSTEN and EKSTRÖM (1971) report compositions of coexisting magnetites, Ca-amphiboles (hornblende and actinolite), and biotites from a metamorphosed iron formation. Magnetites are nearly pure Fe_3O_4. Temperature and pressure conditions of metamorphism were homogeneous, whereas fO_2 and whole-rock composition are variable throughout the formation. Temperature is estimated at ~500°C (ANNERSTEN, pers. comm.). Mn-Fe partitioning for all pairs mineral/magnetite

Table 3. List of values for $Kd = (Mn/Fe)^{fl}/(Mn/Fe^{2+})^{min}$

	800°C	725°C	700°C		
	B	Hd	F	B	P-F
garnet					0.61 ± 0.07
ilmenite		4.4 ± 0.2	3.1 ± 0.2		
cpx	3.0		5.5 ± 1.7	2.4	
	2.3–3.9			1.9–3.3	
amphibole			6.9 ± 2.0		
biotite		17.1 ± 2.7	16.5 ± 5.4		

Errors are reported as 95% confidence intervals. Range of data given for B. Kd'(fl/mt) from ILTON and EUGSTER (1989) combined with Kd(min/mt) from B: BURTON *et al.* (1982); P-F: Kd(garn/ilm) from POWNCEBY *et al.* (1987) combined with Kd(ilm/mt) from F; F: FERRY (1985b); Hd: HILDRETH (1977).

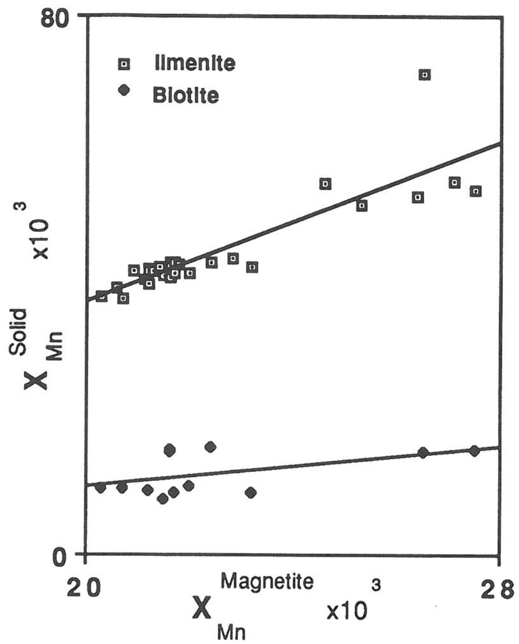

FIG. 2. Mole fraction diagram illustrating Mn-Fe^{2+} partitioning between magnetite, and the minerals ilmenite and biotite. The compositions of the minerals are reported as the mole fraction X_{Mn} = Mn/(Mn + Fe^{2+}). Solid lines mark the partitioning curves for the mean *Kd* associated with each mineral. Mineral compositions are from HILDRETH (1977) for $T \approx$ 720–730°C.

is illustrated in Fig. 3. If one excludes the points in brackets, which represent magnetites contaminated by sphene, then the scatter is greatly reduced and the plot suggests that Mn-Fe exchange equilibria have been approached. *Kd*(min/mt) values are listed in Table 2. ANNERSTEN and EKSTRÖM conclude, based on a broader data set, that the rocks approached chemical equilibrium. Excluding the contaminated pairs, and combining average *Kds*(min/mt) with *Kd*(mt/fl) yields, at ~500°C, values for *Kd*(fl/min) listed in Table 4. *Kd*(fl/hbl) and *Kd*(fl/act) are significantly different (see appendix). The presence of fO_2 gradients and variable Fe/Mg in the silicates neither noticably effect Mn-Fe partitioning between magnetite and the silicates nor among the silicates.

FERRY (1985a) reports compositions of coexisting magnetite (nearly pure Fe_3O_4), biotite, chlorite, talc and calcite from hydrothermally altered gabbro. *Kd*(min/mt) values are given in Table 1. The associated 95% confidence intervals are greater than 100% of the partition coefficients, primarily because of very small sample sizes (*i.e.*, 2–3). *Kd*(calcite/mt) and *Kd*(biotite/mt) are derived from only one sample. The temperature of alteration is estimated at roughly 450–550°C. Combination of *Kd*(mt/fl), at 500°C, with *Kd*(mt/min) yields *Kd*$(Mn/Fe)^{fl}/(Mn/Fe^{2+})^{min}$. The results, listed in Table 4, suggest that lower temperature hydrothermal alteration assemblages likewise favorably partition manganese into the fluid relative to iron. The derivations, although not strictly comparable, are consistent with bulk Mn-Fe partitioning described in basalt-seawater experiments (see introduction for reference list), and with the enrichment of manganese relative to iron in fluids associated with mid ocean ridge hydrothermal systems (SKINNER, 1979). Although these derivations are not complicated by impurities in magnetite, there is insufficient data to suggest the establishment of exchange equilibrium. Furthermore, the results are statistically inconclusive because of small sample sizes. Much more data is needed on such assemblages.

Comparison of the low with the high temperature derivations is complicated by a significant Fe_2TiO_4 component in the high temperature magnetites. Since charge balance effects have been screened by calculating Mn-Fe^{2+} exchange reactions where necessary, only possible structural effects remain. Indirect evidence comes from the compositions of magnetite-hematite assemblages in a regionally metamorphosed quartzite. The assemblages re-

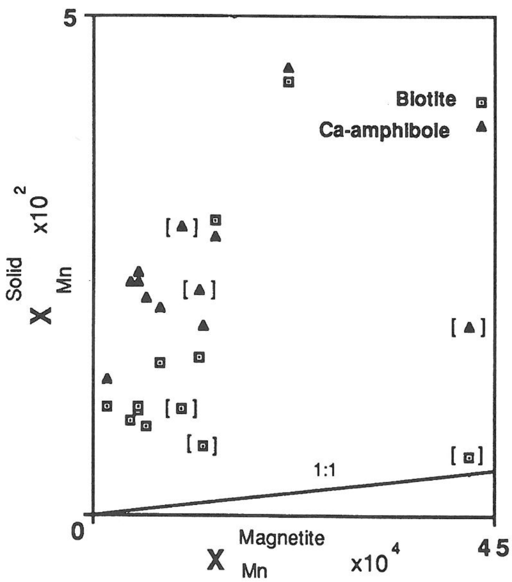

FIG. 3. Mole fraction diagram illustrating Mn-Fe partitioning between magnetite, and the minerals Ca-amphibole and biotite, at ~500°C, where X_{Mn} = Mn/(Mn + Fe). Points in brackets indicate that magnetite is contaminated with sphene. The solid line marks equal partitioning. Mineral compositions are from ANNERSTEN and EKSTRÖM (1971).

Table 4. List of values for $Kd = (M/Fe)^{fl}/(M/Fe)^{min}$ at ~500°C, where M represents the moles of the metal of interest

	Mn-Fe			Zn-Fe			
	F			1	2	Cd-Fe	Cu-Fe
amphibole	4.3*	3.0A ± 1.6	7.0H ± 4.0	70 ± 38	20 ± 15	1160*	11300*
biotite	23*	6.2 ± 3.4		40.3 ± 7.6		1550*	3550*
chlorite	7.7*						
talc	7.3*						
calcite	2.0*						

Errors are 95% confidence intervals. F: *Kd*(fl/mt) from ILTON and EUGSTER (1989) combined with *Kd*(min/mt) from (FERRY, 1985a). *Kd*(biot/fl) for Zn-Fe partitioning from experiments (ILTON, 1987). All other values derived by combining partition coefficients from Table 2 (data from ANNERSTEN and EKSTRÖM, 1971) with *Kd*(fl/mt-annite). Explanation of values 1 and 2 for *Kd*(fl/amph) is given in text.

* Values are statistically inconclusive, see text.

corded fO_2 gradients in the rock, whereas temperature and pressure were homogeneous (RUMBLE 1973; RUMBLE and DICKENSON, 1986). RUMBLE (1973) notes that the systematic partitioning of elements between oxide phases suggests that chemical equilibrium was attained. Magnetite compositions are nearly pure Fe_3O_4 and constant, whereas wt% TiO_2 in the coexisting hematites is variable. $Kd = (Mn/Fe^{2+})^{mt}/(Mn/Fe^{2+})^{hem}$ varies from 1.2 to 46 as wt% TiO_2 in hematite decreases from a high of 16.1 to 3.89. Calculation of *Kd*(hem/mt) with total iron increases the variance fourfold. The change in hematite/fluid partitioning is attributed to variable X_{Ti}^{hem} because magnetite compositions are fairly constant. This suggests that manganese follows titanium, in hematite, for structural reasons as well as for charge balance. DASGUPTA (1967) offers crystal chemical reasons for the correlation of titanium and manganese in magnetite. It is possible that higher concentrations of titanium in magnetite may decrease $(Mn/Fe)^{fl}/(Mn/Fe^{2+})^{mt}$ and that derived $(Mn/Fe)^{fl}/(Mn/Fe^{2+})^{min}$ values, at 700°C, are perhaps too high.

Experimental work, by BURTON *et al.* (1982), on the reaction clinopyroxene = andradite + magnetite + quartz provides further constraints on high temperature mineral-fluid partitioning. BURTON *et al.* (1982) suggest that manganese distribution closely approached equilibrium at 700° and 800°C, but not at 600°C. Product clinopyroxene compositions range from $hd_{87}jo_{13}$ to $hd_{89}jo_{11}$, whereas magnetite is nearly pure Fe_3O_4 with minor manganese. *Kd*(cpx/mt) values are given in Table 1. Combination of *Kd*(mt/cpx) with *Kd*(fl/mt), at 700 and 800°C, yields *Kd*(fl/cpx) values listed in Table 3. Ln *Kd*(fl/cpx), along with the variance in the data, is plotted *v.s.* $1/T$ in Fig. 4. Neglecting the point at 600°C (non equilibrium), and assuming constant ΔH of reaction, yields $\ln Kd(\text{fl/cpx}) = -2073/T(\text{K}) + 3.04$. Given the uncertainties, this temperature dependence should be viewed cautiously. Such a temperature dependence, however, implies that fluids of identical compositions can impart higher $(Mn/Fe)^{cpx}$ ratios at lower temperatures. This may have interesting consequences for interpreting the mineralogy of some metasomatic skarns (*e.g.*, MEINERT, 1987).

Kd(fl/cpx), at 700°C, is lower than the value obtained from FERRY (1985b). This is consistent with the hypothesis that *Kd*s(fl/min) derived from natural magnetites containing significant titanium, are too high. Although *Kd*s derived from BURTON *et al.* (1982) are better contrained than those derived from natural assemblages, a strict comparison of the data sets is compromised by differences in clinopyroxene compositions.

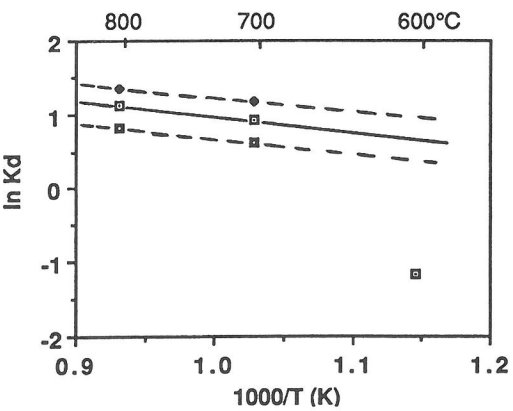

FIG. 4. Ln *Kd v.s.* $1/T$ plot for Mn-Fe partitioning between clinopyroxene and a chloride-rich fluid. The solid line is calibrated to the points at 700°C and 800°C, whereas the point at 600°C has not achieved equilibrium. The dashed lines mark the range of the data. See text for details. Data for cpx-mt taken from BURTON *et al.* (1982).

Summary

The data suggest that Mn-Fe exchange reactions between minerals can approach equilibrium in nature (see ILTON, 1987, for an extensive review of mineral/mineral partitioning). It is, therefore, reasonable to assume that equilibrium Mn-Fe partitioning between minerals and hydrothermal fluids is a viable natural process. More specifically:

(1) Mn-Fe partitioning between minerals varies by over an order of magnitude. This implies that mineral/fluid partitioning should also vary widely. Combination of *Kd*(min/mt) with *Kd*(fl/min) yields a host of mineral/fluid exchange reactions that are distinct and that do vary considerably. This in turn implies that the Mn/Fe compositions of hydrothermal/metamorphic fluids can be strongly influenced by silicate-oxide mineralogy. Tables 3 and 4 are summaries of *Kd*(fl/min) values.

(2) Solubility studies by BOCTOR (1985) suggest that Mn-endmembers are generally more soluble than Fe^{2+}-endmembers under similar conditions. This is consistent with the mt/fl experiments in ILTON and EUGSTER (1989) and with the majority of *Kd*(fl/min) values derived in this paper. Within the statistical error of these calculations, however, almandine/spessartine-garnet may partition manganese into the *solid* phase relative to iron.

(3) The accuracy of derived mineral/fluid exchange reactions may be compromised by uncertain temperature estimates, compositional effects, and lack of definitive proof of exchange equilibrium. Of particular concern are the compositions of natural magnetites which can contain considerable TiO_2. At 700°C, significant titanium in magnetite yielded *Kds*(fl/min) that are possibly too high. Although the 700°C derivations, using natural assemblages (*i.e.,* FERRY, 1985b; HILDRETH, 1977 and 1979), are semi-quantitative, the *relative* behavior of the minerals are consistent. Note that direct comparisons of minerals in the laboratory with those in nature will always be compromised by compositional differences. At lower temperatures, where magnetite compositions are nearly pure Fe_3O_4, the derivations assume greater accuracy given fair temperature estimates and equilibrium.

Zn-Fe PARTITIONING

The existence of zincian biotite (FRONDEL and ITO, 1966), zincian serpentine (BADELOW, 1958), and zincian amphiboles (KLEIN and ITO, 1968) suggests that trace and minor concentrations of zinc will occupy regular octahedral sites in the hydrous silicates. Table 30-D-1 from WEDEPOHL (1972) indicates that the majority of crystal chemical properties of Zn^{2+} are much closer to those of Fe^{2+} than Mg^{2+}. This suggests that Zn^{2+} should substitute for Fe^{2+} preferentially. Alternatively, TAUSON and KRAVECHENKO (1956) claim that a portion of the zinc associated with silicates such as biotite is extra-structural. If true, this "extra-structural" zinc may have "exolved" at very low temperatures, and may not be representative of high temperature hydrothermal processes. Since the available data does not distinguish between Fe^{2+} and Fe^{3+}, distribution coefficients are formulated as Zn-Fe exchange reactions. This is not considered a significant problem since magnetite compositions in the ensuing calculations are nearly pure Fe_3O_4 (*i.e., Kd*(fl/mt) from ILTON and EUGSTER, 1989, is employed, instead of *Kd'*(fl/mt)).

There is far less data on the zinc contents of coexisting minerals than for manganese. One may also assume less accuracy for zinc measurements compared to manganese since zinc is usually a trace element in average rock-forming minerals. Values for $Kd = (Zn/Fe)^{min}/(Zn/Fe)^{mt}$ and $Kd = (Zn/Fe)^{biot}/(Zn/Fe)^{amph}$ derived from mineral compositions in ANNERSTEN and EKSTRÖM (1971), are plotted in Figs. 5 and 6, respectively, and listed in Table 2 (see appendix and previous section for petrological details). *Kd*(silicate/mt) values for zinc are considerably more variable than those for manganese. Zn/Fe tends to be higher in biotite and amphibole relative to magnetite. *Kd*(biot/amph) values exhibit much better precision than *Kd*(silicate/mt) values (see Table 2).

Two values for *Kd*(biot/mt) are given in Table 2. Value 1 encorporates all the data, whereas value 2 excludes two data points that are associated with very low Fe/Mg ratios in biotite. Value 2 is considerably more precise than value 1. There is insufficient data, however, to verify a correlation between *Kd*(biot/mt) and biotite composition. *Kd*(biot/mt) is excluded from further consideration. Instead, an experimentally determined value for *Kd*(biot/fl), from ILTON (1987), is given in Table 4 and used in the ensuing derivations. *Kd*(biot/fl) values are plotted in Fig. 7. The data are preliminary and unreversed (perhaps maximum values). Furthermore, biotite in the experimental assemblage is annite, whereas biotite in the natural assemblage is a Fe-Mg solid solution.

On these cautionary notes, *Kd*(amph/mt) and *Kd*(amph/biot) are combined with *Kd*(fl/mt) and *Kd*(fl/annite), respectively, to yield *Kd*(fl/amph) values listed in Table 4. Values 1 and 2 are derived via *Kd*(amph/biot) and *Kd*(amph/mt), respectively.

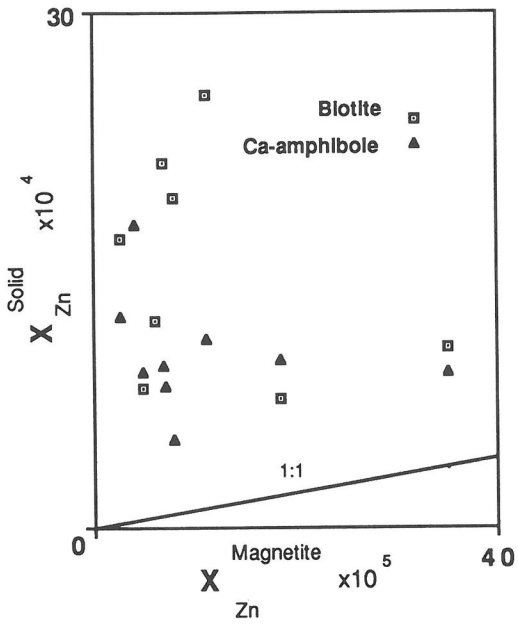

FIG. 5. Mole fraction diagram illustrating Zn-Fe partitioning between magnetite, and the minerals biotite and Ca-amphibole, at ~500°C, where X_{Zn} = Zn/(Zn + Fe). The solid line marks equal partitioning. Mineral compositions from ANNERSTEN and EKSTRÖM (1971).

The results are similar, given their associated uncertainties.

Comparison of the natural data to the magnetite/fluid and annite/fluid experiments suggests that biotite and amphibole should strongly partition zinc into the fluid relative to iron. One might expect minerals with similar octahedral sites, such as chlorite and pyroxene, to exhibit not too disimilar partitioning behavior.

Cd-Fe PARTITIONING

The geochemistry of cadmium is not well understood. The low concentrations of cadmium, in all rock types, accentuates analytical problems. Whereas zinc is usually reported in the ppm range, cadmium is reported at the ppb concentration level (see HEINRICHS *et al.*, 1980, Table 6). According to HEINRICHS *et al.* (1980, Table 5) cadmium is most closely correlated with zinc (ultramafic rocks), magnesium (mafic rocks), zinc (granitic and gneissic rocks), and iron (sedimentary rocks). The similarity in ionic radius for both Cd^{2+} and Ca^{2+} has suggested to some the possibility of a Cd-Ca substitution. VINCENT and BILEFIELD (1960), however, state that "Cadmium appears in the ordinary minerals of the gabbros to follow iron rather than calcium . . . neither does cadmium in the Skaergaard example show any chalcophile tendency." On the other hand, for acidic rocks, DOSTAL *et al.* (1979) claim that "feldspars (especially plagioclase) have the highest content of cadmium." Whereas HEINRICHS *et al.* (1980) state that "Cadmium has a distinct affinity for the six-coordinated Fe^{2+}-Mg sites in biotite, chlorite, and pyroxene . . . cadmium does not replace calcium preferentially in its silicates and in apatite."

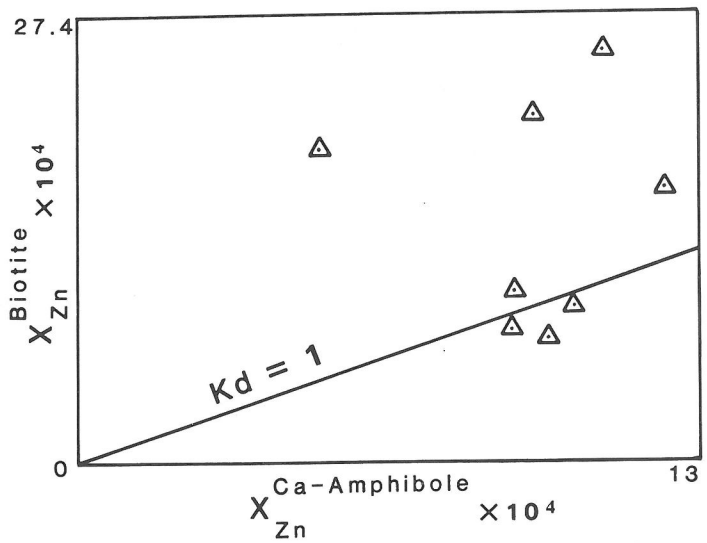

FIG. 6. Mole fraction diagram illustrating Zn-Fe partitioning between biotite and Ca-amphibole, at ~500°C, where X_{Zn} = Zn/(Zn + Fe). The solid line marks equal partitioning. Mineral compositions from ANNERSTEN and EKSTRÖM (1971).

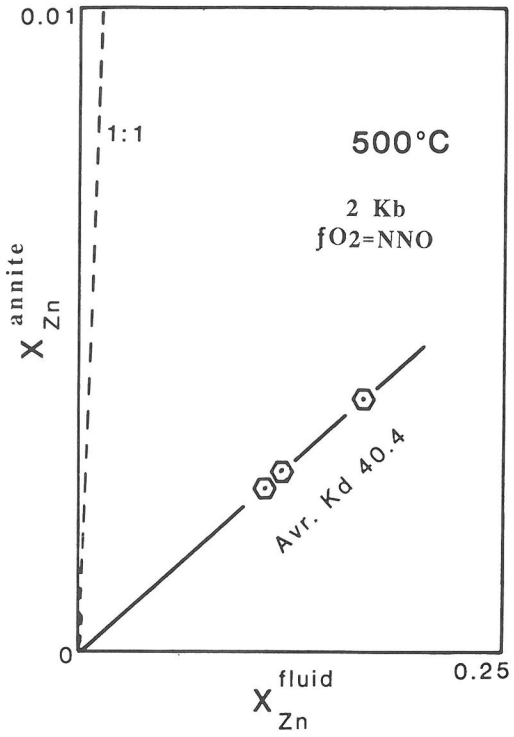

FIG. 7. Mole fraction diagram illustrating experimental Zn-Fe partitioning between annite and a 2 mol chloride solution at 500°C, 2 kb, and fO_2 = NNO. The hexagons represent the experimental distribution coefficients. Average *Kd*(exp) = 40, where $Kd = (Zn/Fe)^{fl}/(Zn/Fe)^{biot}$. Data from ILTON (1987).

HAACK *et al.* (1984) conclude that the Cd-Ca controversy is still unresolved.

ANNERSTEN and EKSTRÖM (1971) report the concentration of cadmium in coexisting magnetite, biotite and Ca-amphibole (see appendix and Mn-Fe section for petrological details). *Kd*(min/mt) values are listed in table 2 and illustrated in Fig. 8. Analytical difficulties and variable silicate compositions may have increased the variance of the data. There is insufficient data, however, to test the latter possibility. Despite the scatter, the data describe the tendency for cadmium to partition preferentially, with respect to iron, into biotite and Ca-amphibole relative to magnetite. Cd-Fe partitioning is considerably more systematic between biotite and amphibole (see Fig. 9 and Table 2). Since cadmium is extremely partitioned into the fluid relative to magnetite at 700°C (ILTON and EUGSTER, 1989), we assume that cadmium is partitioned *at least* as strongly at 500°C (although the experiments are unreversed). This is a fair assumption since the primary reason for such behavior is the relatively large size of the cadmium ion. Given this assumption, and assuming a Cd-Fe exchange, combination of *Kd*(fl/mt) with average *Kd*(mt/min) yields *Kd*(fl/min) values listed in Table 4. Although the partition coefficients indicate that biotite and amphibole should very strongly partition cadmium into the fluid relative to iron, large uncertainties associated with the experiments and natural assemblages render the results statistically inconclusive.

Cu-Fe PARTITIONING

One might expect Cu^{2+} to preferentially substitute for Fe^{2+} in minerals such as biotite (Cu^{1+} will be discussed later). ILTON (1987) detected weak correlations between iron and copper in biotites and amphiboles, whereas GRAYBEAL (1973) and HAACK *et al.* (1984) found no correlation between copper and any of the major elements. Copper's preference for distorted octahedral sites (the Jahn Teller effect), and the possible presence of submicroscopic sulfide inclusions in silicates complicates its geochemistry.

Despite the uncertainties, mineral analyses from ANNERSTEN and EKSTRÖM (1971) were used to estimate the partitioning of copper and iron between magnetite, and Ca-amphibole and biotite (see appendix and Mn-Fe section for petrological details).

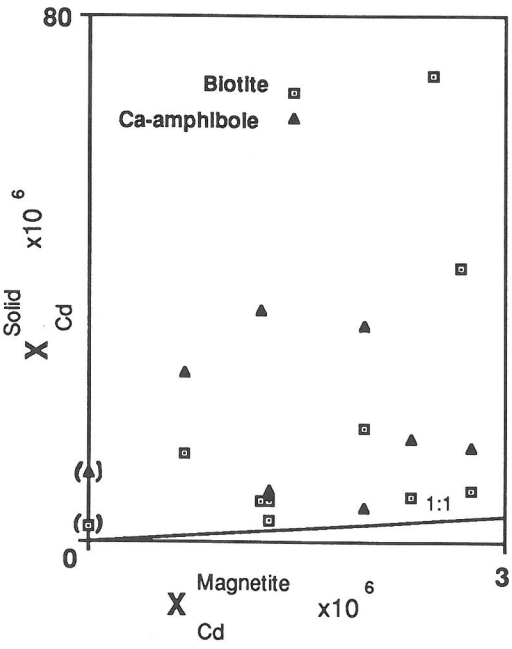

FIG. 8. Mole fraction diagram illustrating Cd-Fe partitioning between magnetite, and the minerals biotite and Ca-amphibole, at ~500°C, where X_{Cd} = Cd/(Cd + Fe). Points in parentheses were judged anomalous. The solid line marks equal partitioning. Mineral compositions from ANNERSTEN and EKSTRÖM (1971).

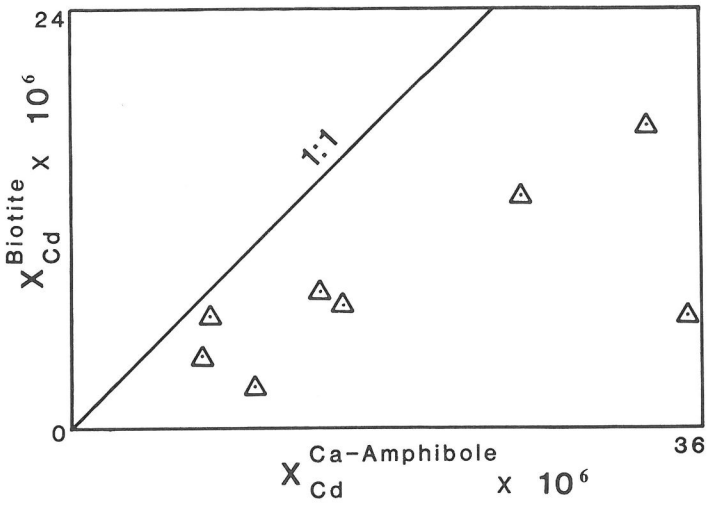

FIG. 9. Mole fraction diagram showing Cd-Fe partitioning between biotite and Ca-amphibole, at ~500°C, where X_{Cd} = Cd/(Cd + Fe). The solid line marks equal partitioning. Mineral compositions from ANNERSTEN and EKSTRÖM (1971).

Kd(min/mt) values are illustrated in Fig. 10 and listed in Table 2. As expected the data shows considerable scatter. The data suggest that copper, relative to iron, has a tendency to be preferentially partitioned into biotite and Ca-amphibole relative to magnetite. *Kd*(biot/mt) exhibits the greatest variance. If two values for *Kd*(biot/mt), associated with very low Fe/Mg ratios, are excluded from the mean, then the precision is considerably enhanced (value 1 *v.s.* value 2 in Table 2). There is insufficient data, however, to test for a correlation between *Kd*(biot/mt) and biotite composition. Assuming a Cu-Fe exchange and combining *Kd*(mt/fl) with *Kd*(mt/min), given that *Kd*(mt/fl) is insensitive to temperature within experimental error (ILTON and EUGSTER, 1989) yields *Kds*(fl/min) values listed in Table 4.

The derivations suggest that biotite and Ca-amphibole, as well as magnetite extremely partition copper into the fluid relative to iron. Propagation of errors associated with *Kd*(fl/mt) and *Kd*(min/mt), however, indicate that *Kd*(fl/min) values are statistically inconclusive.

A further complication involves the significance and nature of the copper species in these silicates. ILTON and VEBLEN (1988a,b) used TEM methods to show that *anomalous* copper (≥ ~500 ppm) in biotites from rocks associated with porphyry copper deposits could be accounted for by submicroscopic inclusions of native copper along the interlayers. Textural evidence suggested that copper may have substituted for K^+ in the interlayer sites, *perhaps* during hydrothermal activity or incipient weathering, prior to reduction and precipitation to native copper. Although the biotites used in this study contain only trace concentrations of copper (6–18

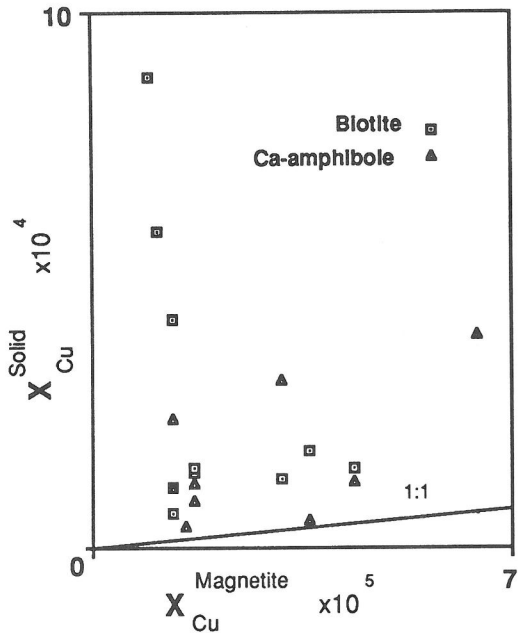

FIG. 10. Mole fraction diagram illustrating Cu-Fe partitioning between magnetite, and the minerals biotite and Ca-amphibole, at ~500°C, where X_{Cu} = Cu/(Cu + Fe). The solid line marks equal partitioning. Mineral compositions from ANNERSTEN and EKSTRÖM (1971).

ppm) and probably have not experienced the same history as the biotites studied by ILTON and VEBLEN (1988a,b), the TEM evidence questions the assumption that copper substitutes for octahedrally coordinated iron in porphyry copper environments. Such evidence is consistent with observations that Cu^{1+}, not Cu^{2+}, is the dominant oxidation state of copper in the hypogene environment (CANDELA and HOLLAND, 1984; WEDEPOHL, 1974).

CONCLUSION

The partition coefficients derived in this contribution and in EUGSTER and ILTON (1983) for Mg-Fe, indicate that the common rock-forming silicates and oxides tend to partition (Cu > Cd) ⩾ Zn ⩾ Mn ⩾ Fe ⩾ Mg into chloride-rich hydrothermal/metamorphic fluids. A possible exception for manganese is almandine-garnet. Copper and cadmium are bracketed because the 95% confidence intervals exceed 100% of their associated partition coefficients. The results for copper and cadmium are intriguing but, we must conclude, statistically inconclusive.

The partition coefficients contain information on the relative mobility of these base metals. Note that, in general, the less abundant the base metal the greater its partitioning into the fluid. In Part II (ILTON, 1990), the partition coefficients are used in a simple fluid flow model to demonstrate that, under certain conditions, congruent exchange reactions can strongly fractionate the base metals, and enrich the geochemically scarce base metals relative to iron.

The partition coefficients are preliminary values, subject to revision by further experimental work and greater information concerning base metals in naturally occurring silicates and oxides. Our knowledge is still extremely limited on both accounts.

Acknowledgements—We thank our colleagues Siggi Gislason and Glenn Wilson for many fruitful discussions. Hans Annersten and John Ferry provided constructive reviews of an early version of the manuscript. ESI thanks Phil Candela, and Lukas Baumgartner for constructive reviews and comments. This research was funded, in part, by NSF grants EAR-8206177 and EAR-8411050 awarded to Hans P. Eugster.

REFERENCES

ANNERSTEN H. and EKSTRÖM T. (1971) Distribution of major and minor elements in coexisting minerals from a metamorphosed iron formation. *Lithos* **4,** 185–204.

BADELOW S. T. (1958) Pyrochroit, zinkhaltiger serpentin und allophan aus der Lagerstätte Almalyk (Usbekistan). *Sapiski Wsesojusn. Miner. Obsch.* **87,** 698.

BANKS N. G. (1974) Distribution of copper in biotite and biotite alteration products in intrusive rocks near two Arizona porphyry copper deposits. *J. Res. U.S. Geol. Surv.* **2,** 195–211.

BARNES H. L. (1979) Solubilities of ore minerals. In *Geochemistry of Hydrothermal Ore Deposits* (ed. H. L. BARNES), pp. 404–454. John Wiley & Sons.

BISCHOFF J. L. and DICKSON F. W. (1975) Seawater-basalt interaction at 200°C and 500 bars: implications for origin of seafloor heavy metal deposits and regulation of seawater chemistry. *Earth Planet. Sci. Lett.* **25,** 385–397.

BOCTOR N. Z. (1985) Rhodonite solubility and thermodynamic properties of aqueous $MnCl_2^0$ in the system $MnO\text{-}SiO_2\text{-}HCl\text{-}H_2O$. *Geochim. Cosmochim. Acta* **49,** 565–575.

BURTON J. C., TAYLOR L. A. and CHOU I-M. (1982) The fO_2-T and fS_2-T stability relations of hedenbergite and hedenbergite-johannsenite solid solutions. *Econ. Geol.* **77,** 764–783.

CANDELA P. A. and HOLLAND H. D. (1984) The partitioning of copper and molybdenum between silicate melts and aqueous fluids. *Geochim. Cosmochim. Acta* **48,** 373–380.

DASGUPTA H. C. (1967) Intracrystalline element correlation in magnetite. *Econ. Geol.* **62,** 487–493.

DE ALBUQUERQUE C. A. R. (1971) Petrochemistry of a series of granitic rocks from northern Portugal. *Bull. Geol. Soc. Amer.* **82,** 2738–2798.

DE ALBUQUERQUE C. A. R. (1973) Geochemistry of biotites from granitic rocks, northern Portugal. *Geochim. Cosmochim. Acta* **37,** 1799–1802.

DISSANAYAKE C. B. and VINCENT E. A. (1972) Zinc in rocks and minerals from the Skaergaard intrusion, east Greenland. *Chem. Geol.* **9,** 285–297.

ELLIS A. J. (1968) Natural hydrothermal solutions and experimental hot-water/rock interaction: Reactions with NaCl solutions and trace metal extraction. *Geochim. Cosmochim. Acta* **32,** 1356–1363.

EUGSTER H. P. (1986) Minerals in hot water. *Amer. Mineral.* **71,** 655–673.

EUGSTER H. P. and ILTON E. S. (1983) Mg-Fe fractionation in metamorphic environments. In *Kinetics and Equilibrium in Mineral Reactions* (ed. S. K. SAXENA), pp. 115–140. Springer-Verlag.

FERRY J. M. (1985a) Hydrothermal alteration of Tertiary igneous rocks from the Isle of Skye, northwest Scotland I. Gabbros. *Contrib. Mineral. Petrol.* **91,** 264–282.

FERRY J. M. (1985b). Hydrothermal alteration of Tertiary igneous rocks from the Isle of Skye, northwest Scotland II. Granites. *Contrib. Mineral. Petrol.* **91,** 283–304.

FRONDEL C. and ITO J. (1966) Hendricksite, a new species of mica. *Amer. Mineral.* **51,** 1107.

GRAYBEAL F. T. (1973) Copper, manganese, and zinc in coexisting mafic minerals from Laramide intrusive rocks in Arizona. *Econ. Geol.* **68,** 785–798.

HAACK U., HEINRICHS H., BONEB M. and SCHNEIDER A. (1984) Loss of metals from pelites during regional metamorphism. *Contrib. Mineral. Petrol.* **85,** 116–132.

HAJASH A. (1975) Hydrothermal processes along mid-ocean ridges: an experimental investigation. *Contrib. Mineral. Petrol.* **53,** 205–226.

HASLAM H. W. (1968) The crystallization of intermediate and acid magmas at Ben Nevis, Scotland. *J. Petrol.* **9,** 84–104.

HEINRICHS H., SCHULZ-DOBRICK B. and WEDELPOHL K. H. (1980) Terrestrial geochemistry of Cd, Bi, Tl, Pb, Zn, and Rb. *Geochim. Cosmochim. Acta.* **44,** 1519–1533.

HENDRY D. A. F., CHIVAS A. R., REED S. J. B. and LONG J. V. P. (1981) Geochemical evidence for magmatic fluids in porphyry copper mineralization. Part II. Ion probe analysis of Cu contents of mafic minerals, Koloula igneous complex. *Contrib. Mineral. Petrol.* **78,** 404–412.

HENLEY R. W. and ELLIS A. J. (1983) Geothermal systems ancient and modern: a geochemical review. *Earth-Science Rev.* **19,** 1–50.

HILDRETH E. W. (1977) The magma chamber of the Bishop Tuff: Gradients in temperature, pressure and composition. Ph.D. thesis. University of California, Berkeley, California. 328p.

HILDRETH E. W. (1979) The Bishop Tuff: Evidence for the origin of compositional zonation in silicic magma chambers. *Geol. Soc. Amer. Spec. Paper* 180, 43–75.

HOLLAND H. D. (1972) Granites, solutions and base metal deposits. *Econ. Geol.* **67,** 281–301.

ILTON E. S. (1987) Base metal exchange between rock-forming silicates, oxides, and hydrothermal/metamorphic fluids. Ph.D. Dissertation. Johns Hopkins University, Baltimore, Maryland. 230p.

ILTON E. S. (1990) Partitioning of base metals between silicates, oxides, and a chloride-rich hydrothermal fluid. Part II. Some aspects of base metal fractionation during isothermal metasomatism. In *Fluid-Mineral Interactions: A Tribute to H. P. Eugster* (eds. R. J. SPENCER and I-MING CHOU), Spec. Publ. 2, pp. 171–177. The Geochemical Society.

ILTON E. S. and EUGSTER H. P. (1989) Base metal exchange between magnetite and a chloride-rich hydrothermal fluid. *Geochim. Cosmochim. Acta* **53,** 291–301.

ILTON E. S. and VEBLEN D. R. (1988a) Cu in sheet silicates from rocks associated with porphyry copper deposits: A transmission electron microscopy study. (abstr.). *The V. M. Goldschmidt Conference-Symposiom: Ore-Forming Processes.* The Geochemical Society. Abstracts and Program, p. 49.

ILTON E. S. and VEBLEN D. R. (1988b) Cu inclusions in sheet silicates from porphyry copper deposits. *Nature* **334,** 516–518.

KLEIN C. and ITO J. (1968) Zincian and manganoan amphiboles from Franklin, New Jersey. *Amer. Mineral.* **53,** p. 1264.

MAROWSKY G. and WEDEPOHL K. H. (1971) General trends in the behavior of Cd, Hg, Tl and Bi in some major rock forming processes. *Geochim. Cosmochim. Acta* **35,** 1255–1267.

MEINERT L. D. (1987) Skarn zonation and fluid evolution in the Groundhog Mine, Central Mining District, New Mexico. *Econ. Geol.* **82,** 523–545.

MOTTL M. J., HOLLAND H. D. and CORR R. F. (1979) Chemical exchange during hydrothermal alteration of basalt by seawater–II Experiments for Fe, Mn and sulfur species. *Geochim. Cosmochim. Acta* **43,** 869–884.

POWNCEBY M. I., WALL V. J. and O'NEILL H. ST. C. (1987) Fe-Mn partitioning between garnet and ilmenite: experimental calibration and applications. *Contrib. Mineral. Petrol.* **97,** 116–126.

ROEDDER E. (1984) *Fluid Inclusions.* Reviews in Mineralogy 12. 643pp. Mineralogical Society of America.

RUMBLE D. (1973) Fe-Ti oxide minerals from regionally metamorphosed quartzites of western New Hampshire. *Contrib. Mineral. Petrol.* **42,** 181–195.

RUMBLE D. and DICKENSON M. P. (1986) Field trip guide to black mountain Wildwood road cut and Beaver Brook, Mount Moosilauke area, New Hampshire. *Field Trip Guide Book: Regional Metamorphism and Metamorphic Relations in N. Western and Central New England.*

SEYFRIED W. E. and BISCHOFF, J. L. (1981) Experimental seawater-basalt interaction at 300°C, 500 bars, chemical exchange, secondary mineral formation and implications for the transport of heavy metals. *Geochim. Cosmochim. Acta* **46,** 985–1002.

SEYFRIED W. E. and JANECKY D. R. (1985). Heavy Metal and sulfur transport during subcritical and supercritical hydrothermal alteration of basalt; influence of fluid pressure and basalt composition and crystallinity. *Geochim. Cosmochim. Acta* **49,** 2545–2560.

SEYFRIED W. E. and MOTTL M. J. (1982) Hydrothermal alteration of basalt by seawater under seawater-dominated conditions. *Geochim. Cosmochim. Acta* **46,** 985–1002.

SKINNER B. J. (1979) The many origins of hydrothermal mineral deposits. In *Geochemistry of Hydrothermal Ore Deposits,* (ed. H. L. BARNES), pp. 1–21. J. Wiley & Sons.

SVERJENSKY D. A. (1984) Prediction of Gibbs free energies of calcite-type carbonates and the equilibrium distribution of trace elements between carbonates and aqueous solutions. *Geochim. Cosmochim. Acta* **48,** 1127–1134.

SVERJENSKY D. A. (1985) The distribution of divalent trace elements between sulfides, oxides, silicates and hydrothermal solutions: I. Thermodynamic basis. *Geochim. Cosmochim. Acta* **49,** 853–864.

TAUSON L. V. and KRAVCHENKO L. A. (1956) Characteristics of lead and zinc distribution in minerals of the Caledonian granitoids of the Susamyr batholith in central Tian-Shan. *Geochemistry* **1,** 78–88.

VINCENT E. A. and BILEFIELD L. I. (1960) Cadmium in rocks and minerals from the Skaergaard intrusion, East Greenland. *Geochim. Cosmochim. Acta* **19,** 63–69.

WEDEPOHL K. H. (1972) Zinc. In *Handbook of Geochemistry* (ed. K. H. WEDEPOHL), p. 30-D-3. Springer-Verlag.

WEDEPOHL K. H. (1974) Copper. In *Handbook of Geochemistry* (ed. K. H. WEDEPOHL), p. 29-D-14. Springer-Verlag.

WEDEPOHL K. H. (1978) Manganese. In *Handbook of Geochemistry* (ed. K. H. WEDEPOHL), p. 25-D-3. Springer-Verlag.

WEISSBERG B. G., BROWNE P. R. L. and SEWARD T. M. (1979) Ore metals in active geothermal systems. In *Geochemistry of Hydrothermal Ore Deposits* (ed. H. L. BARNES), pp. 738–780. John Wiley & Sons.

APPENDIX
MINERAL COMPOSITIONS AND ZONING

FERRY (1985b)

Biotite compositions used in the derivations are iron rich, with Fe/Mg ratios = 2.25–1.14, and Al(VI) poor. Si/Al ratios = 2.65–2.3 and (Si + Al)IV totals are slightly less than 4. Compositional zoning is *not* reported for biotite. Amphiboles are either ferro-hornblende, ferro-edenite, or ferro-edenitic hornblende (nomenclature of Leake, 1978). One sample contains a Na rich amphibole. $Fe^{2+}/(Mg + Fe^{2+}) = 0.56–0.92$. Pyroxenes are ferroaugites with 0.78–0.86 Ca/60 and $Fe^{2+}/(Mg + Fe^{2+}) = 0.65–0.88$.

Chemical zoning was minor for pyroxene and amphibole in most samples. Some biotite, amphibole, and pyroxene have been partially altered to chlorite. The compositions of unaltered and partially altered silicates are identical.

Magnetites are near magnetite-ulvospinel solid solutions, where wt.% TiO_2 = 8.36–15.8. Most magnetites show signs of incipient oxidation-exsolution to submicroscopic intergrowths of ilmenite and magnetite. The process is considered to be isochemical with respect to cations, and averaged compositions are reported. Ilmenites are homogenous (zoning is not reported) and unaltered, with minor Mn and Fe^{3+}. Ferry concludes that the compositions of these minerals were unaffected by later hydrothermal activity and probably record conditions near crystallization temperatures (650–750°C).

Hildreth (1977)

Mineral compositions are broadly similar to those described in Ferry (1985b). Microprobe analyses indicate that magnetite, ilmenite, and biotite are *un*zoned with respect to major elements and Mn.

The majority of individual biotite crystals indicate some degree of inhomogeneity; interlayer cations can vary by 20%, FeO and MgO by ±5–10%, whereas MnO is fairly homogenous. Lower T biotites exhibit varying degrees of oxidation. Biotites in devitrified samples are severely oxidised and iron oxides are present along cleavage planes. Hildreth, however, confined his study to vitric samples. Furthermore, biotite octahedral site compositions are strongly correlated to T and *Kd*(biot/mt) values indicate that Fe and Mn were systematically partitioned between biotite and magnetite (see Table 1 and Fig. 2, this paper). Hildreth concludes that whereas interlayer and hydroxyl sites record post magmatic compositions, octahedral site compositions generally maintain their magmatic signatures (although he warns for a—"cautious approach to the data").

Magnetite and ilmenite compositions are strongly correlated to T. *Kd*(ilm/mt) values indicate that Mn and Fe were systematically partitioned between ilmenite and magnetite. Furthermore, *Kd*(ilm/mt) exhibits a significant T dependence, where *Kd*(720–730°C) = 2.04 and *Kd*(765–790°C) = 1.55. A t-test indicates that the difference between the two *Kd*s is highly significant, where $P \ll 0.001$.

The precision and systematic nature of the data suggests that Mn-Fe partitioning between magnetite, and ilmenite and biotite approached equilibrium. The evidence is stronger for mt-ilm than mt-biot.

Annersten and Ekström (1971)

Magnetites are nearly pure Fe_3O_4. Amphiboles are either hornblende or actinolite with Fe/Mg = 3.6–0.0017. Fe/Mg = 2.0–0.0084 for biotite. The Fe/Mg ratios reflect fO_2 gradients.

Microprobe analyses indicate that biotite and amphibole are chemically homogenous with respect to major elements and Mn. Chemical zoning is *not* reported. Trace element analyses for magnetite (Mn, Zn, Cu, Cd) and both silicates (Zn, Cu, Cd) were obtained from mineral separates and AAS. A few magnetite grains were contaminated by sphene. Mn seemed to be most effected by sphene contamination.

Analysed pairs of biotite and amphibole were in close contact, whereas the textural relationship of mt-silicate pairs was not reported.

Kd(mt/silicate) for Mn-Fe partitioning is largely independent of Fe/Mg, whereas Cd, Zn, and Cu partitioning indicates some correlation to Fe/Mg ratio. Excluding the oxidised samples increases precision, but more data is required to provide an adequate test of this hypothesis. There is a significant difference between *Kd*(hbl/mt) and *Kd*(act/mt) for Mn-Fe partitioning, where a t-test yields $0.05 \gg P > 0.02$.

The large variance in Kd(silicate/mt) for Cd, Zn, and Cu indicates either analytical problems, hidden correlation factors, lack of M-Fe exchange equilibrium, or some combination of the above.

Ferry (1985a)

The pertinent alteration reactions are olivine to talc + magnetite, and talc and magnetite to chlorite or montmorillinite. Magnetite grains are intimately associated with talc and chlorite (Ferry—"magnetite . . . (is) . . . set in a matrix of talc and chlorite). Biotite usually occurs along grain boundaries in close contact with chlorite and amphibole. Amphibole occurs in a variety of textural relationships including as crystals within chlorite. Calcite occurs within plagioclase and along grain boundaries. The exact textural relationships, however, are not given for any one sample. One might assume that magnetites had a better chance of equilibrating with chlorite and talc.

$Fe^{2+}/(Mg + Fe^{2+})$ = 0.03–0.07, 0.23–0.49, 0.20–0.53, and 0.13–0.44 for talc, chlorite, amphibole, and biotite. Amphiboles are primarily actinolites, biotites have low interlayer site occupencies and low Al(VI), chlorites have 1.2–2.5 Al/140, and calcites are nearly pure $CaCo_3$. Zoning and inhomogeneity within single crystals are not reported.

Rumble (1973)

Oxide phases are in intimate contact. Zoning is *not* reported. Hematite often contains submicroscopic-microscopic lamellae of ilmenite. Rumble used a broad electron beam to get a bulk analysis. He reasoned that bulk compositions were representative of homogenous ilmeno-hematite solid solutions at recrystallization conditions.

Burton et al. (1982)

Andradite and magnetite exhibited minor compositional zoning. Clinopyroxene grains were to small for accurate microprobe analysis. Burton *et al.* (1982) calculated run-product clinopyroxene compositions from mass balance.